# Composition-dependent structural properties in ScGaN alloy films: A combined experimental and theoretical study

Costel Constantin, Muhammad B. Haider, David Ingram, and Arthur R. Smith
*Condensed Matter and Surface Science Program, Department of Physics and Astronomy, Ohio University, Athens, Ohio 45701*

Nancy Sandler
*Condensed Matter and Surface Science Program, Department of Physics and Astronomy, Ohio University, Athens, Ohio 45701 and Institut de Ciència de Materials de Barcelona-CSIC, Campus UAB, Barcelona, 08193 Spain*

Kai Sun
*Electron Microbeam Analysis Laboratory, University of Michigan, Ann Arbor, Michigan 48109-2143*

Pablo Ordejón
*Institut de Ciència de Materials de Barcelona-CSIC, Campus UAB, Barcelona, 08193 Spain*

(Received 3 August 2005; accepted 2 November 2005; published online 16 December 2005)

Experimental and theoretical results are presented regarding the incorporation of scandium into wurtzite GaN. Variation of the *a* and *c* lattice constants with Sc fraction in the low Sc concentration regime (0%–17%) are found that can be well explained by the predictions of first-principles theory. The calculations allow a statistical analysis of the variations of the bond lengths and bond angles as functions of Sc concentration. The results are compared to predictions from both a prior experimental study [Constantin *et al.*, Phys. Rev. B **70**, 193309 (2004)] and a prior theoretical study [Farrer and Bellaiche *et al.* Phys. Rev. B **66**, 201203(R) (2002)]. It is found that the ScGaN lattice can be very well modeled as being wurtzitelike but with local lattice distortions arising from the incorporation of the Sc atoms. Effects of the addition of Sc on the stacking order for a large Sc fraction is also studied by high resolution transmission electron microscopy. The results show the existence of stacking faults, and induced stacking disorder. The explanation for the lattice constant variations is based on the effects of local lattice distortions and not related to the stacking faults.
 [DOI: 10.1063/1.2140889]

## I. INTRODUCTION

Dismukes and Moustakas proposed to enhance the potential of GaN for optoelectronic applications by combining it with ScN.[1,2] ScN is known to be a rocksalt (cubic) semiconductor with an indirect band gap from $\Gamma \rightarrow X$ of ~1 eV and a direct transition $E_t$ at the $X$ point of 2.1–2.4 eV.[1,3–7] By combining GaN with ScN, the ScGaN ternary alloys are expected to exhibit novel properties, especially near the boundary between rocksalt and wurtzite phases.[5,9] In principle, the alloy range with Sc concentration from 0% to 100% should allow band gap control over the whole range 2.1–3.4 eV. Takeuchi predicted a metastable wurtzite phase (denoted
*w*-ScN) for ScN.[8] Farrer and Bellaiche found that ScN can form a layered hexagonal phase (*h*-ScN) which should be metastable, whereas the *w*-ScN should be unstable.[9] Experimentally, Little and Kordesch grew ScGaN on a quartz substrate by the sputtering technique.[10] They reported amorphous or microcrystalline films and a linearly decreasing optical band gap (from 3.5 down to 2.0 eV) with increasing Sc concentration. More recently, Constantin *et al.*[11] reported the first evidence for the metastable *h*-ScN phase by studying ScGaN alloys grown over the whole range of concentration between 0% and 100%. It was found that $Sc_xGa_{1-x}N$ alloys are formed for two molecular beam epitaxy growth regimes: low $x$ (0%–17%) and high $x$ (54%–100%). For the high $x$ regime, rocksalt structure is formed. For the low $x$ regime, the wurtzitelike structure is formed, in which an anisotropic expansion of the lattice constants $a$ and $c$ occurs as $x$ increases. The $a$ lattice constant was carefully measured using reflection high energy electron diffraction (RHEED), while the $c$ lattice constant was measured using x-ray diffraction (XRD).[11]

Using these methods, $a$ was found to increase 13 times as much as $c$ over this range 0%–17%, thus resulting in a decrease in the $c:a$ ratio. This decrease compared the best with predictions based on a hexagonal ScN phase as the high $x$ endpoint. Constantin *et al.* explained that this anisotropic lattice constant expansion can be understood in terms of a model in which there occur local lattice distortions of the wurtzite structure in the vicinity of $Sc_{Ga}$ substitutional sites. In particular, as the *out-of-plane* N-Sc-N bond angle decreases, the lattice constant $a$ increases. And by geometry, the *in-plane* N-Sc-N bond angle should increase. For Sc-N and Ga-N bond lengths roughly equal, then this distortion would also result in a decrease of $c$. The slight experimentally observed increase in $c$ for small $x$ is attributed to the larger bond length of Sc-N (e.g., ~2.25 Å in rocksalt ScN) in comparison to Ga-N (e.g., ~1.95 Å in wurtzite GaN). However, in the previous work, neither the bond angles nor the bond lengths were directly determined (measured or predicted), which is necessary to prove the lattice distortion model. In this paper, we report a combined experiment and

 

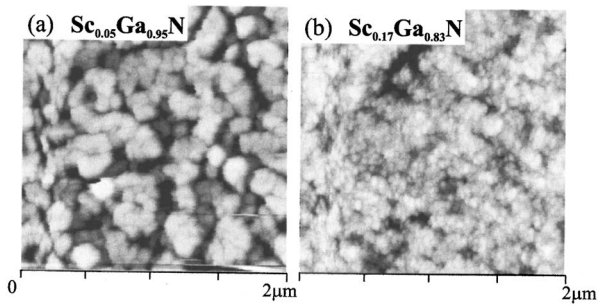


FIG. 1. 2 $\mu$m$\times$2 $\mu$m AFM images of $Sc_xGa_{1-x}N$/GaN/sapphire(0001) with (a) $x=5\%$, and (b) $x=17\%$.

theory study of ScGaN with small Sc concentration only (Sc fraction up to 17%). We present new experimental data resolving the ScGaN lattice along the growth direction and supporting the conclusion that the ScGaN lattice is a crystalline alloy containing substitutional Sc atoms. As well, we observe that, above a certain Sc fraction, there is evidence of defects, most likely in the form of stacking faults. Using first-principles theory, we show that the lattice distortions found in the experiments are reproduced in the calculations and that the distortions arise from bond-angle and bond-length changes in the wurtzitelike lattice. We present calculations for a range of Sc fraction covering the range studied in the experiment.

## II. EXPERIMENT

### A. Experimental methods

The ScGaN films are grown using radio frequency plasma molecular beam epitaxy (rf-plasma MBE) using $N_2$ as a source gas, and employing effusion cells for both Ga and Sc evaporation. The sapphire (0001) substrates are first heated to 900 °C and nitridated for 30 min with the N plasma source operating at 500 W and with a $N_2$ flow rate of 1.1 sccm ($P_{\text{chamber}}=9\times10^{-6}$ Torr). A buffer layer of GaN is then grown at a substrate temperature of 650 °C, under Ga-rich conditions, and to a thickness of 50 nm. Finally, the ScGaN layer is grown at a specific cation flux ratio $r=J_{\text{Sc}}/(J_{\text{Sc}}+J_{\text{Ga}})$, and with a substrate temperature of 650 °C. The ScGaN layers are grown under N-rich conditions ($J_{\text{Sc}}+J_{\text{Ga}}<J_{\text{N}}$). The thickness of the ScGaN layer is in the range 140–200 nm. The growth is monitored *in situ* by RHEED using a 20 keV $e^-$ beam. The films are measured *ex situ* by XRD, atomic force microscopy (AFM), high resolution transmission electron microscopy (HRTEM), and Rutherford backscattering (RBS).

### B. Experimental results

Shown in Fig. 1(a) is a 2 $\mu$m$\times$2 $\mu$m AFM image of $Sc_xGa_{1-x}N$/GaN/sapphire(0001) with $x=5\%$. The surface consists of closely packed hillocks. The root-mean-square (rms) surface roughness is 115 Å with a peak-to-valley height of 875 Å. These results suggests a 3D growth mode, which is consistent with growth under N-rich conditions. As we increased the Sc concentration to $x=17\%$ [Fig. 1(b)], the root-mean-square (rms) surface roughness and the peak-to-valley height are 38.4 Å and 419 Å, respectively—less than that obtained for $x=5\%$. The growth mode, however, is still clearly 3D, and the reduction in roughness is attributed to an increase in surface diffusion barrier, resulting in smaller, more densely-packed grains. The roughness indicated in these AFM images is consistent with the results of RHEED studies in the same composition range (0%–17%), which also indicated 3D growth mode for the ScGaN grown under these conditions.[11] Nonetheless the RHEED patterns indicated a crystalline surface.

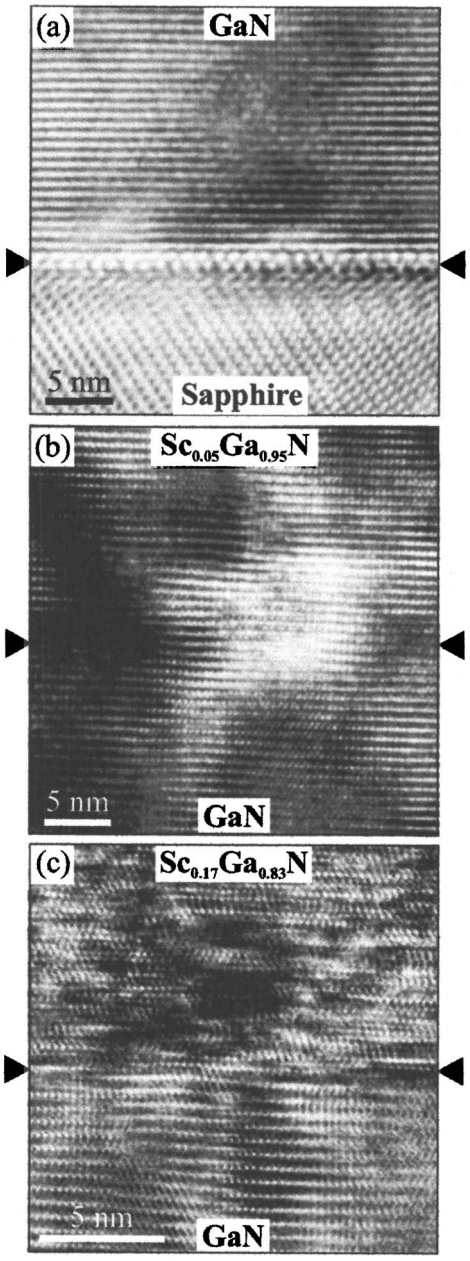


FIG. 2. HRTEM images of sapphire, GaN, and $Sc_xGa_{1-x}N$; (a) 30 nm $\times$30 nm HRTEM image showing well ordered GaN and sapphire crystals; (b) 30 nm$\times$30 nm HRTEM image showing GaN and $Sc_xGa_{1-x}N$ with $x=5\%$; (c) 15 nm$\times$15 nm HRTEM image showing GaN and $Sc_xGa_{1-x}N$ with $x=17\%$ [the black arrows show the interface between GaN and $Sc_xGa_{1-x}N$ layers for figures (b) and (c)].

Figure 2 shows high-resolution TEM (HRTEM) images for $Sc_xGa_{1-x}N$/GaN/sapphire films with $x=5\%$ and 17%.

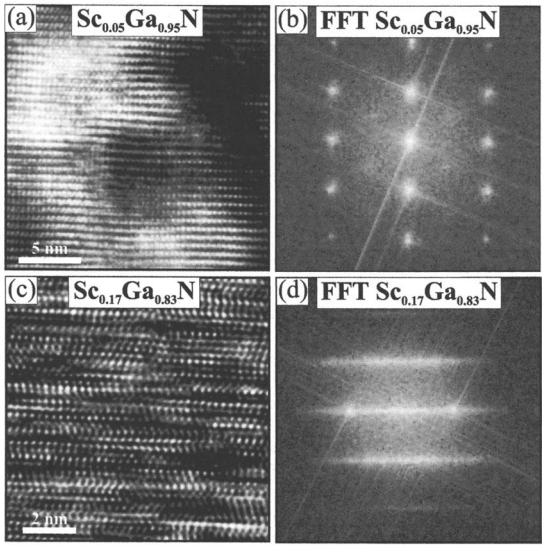


FIG. 3. HRTEM and FFT images of $Sc_xGa_{1-x}N$; (a) 35 nm×35 nm HRTEM image of $Sc_xGa_{1-x}N$ with $x=5\%$; (b) FFT image of (a); (c) 9 nm ×9 nm HRTEM image of $Sc_xGa_{1-x}N$ with $x=17\%$; (d) FFT image of (c).

Figure 2(a) shows the interface between the well ordered GaN and sapphire layers. These layers show a high degree of crystalline perfection. The GaN layer in particular shows the good crystallinity consistent with the Ga-rich buffer layer growth conditions. The interface between the $Sc_xGa_{1-x}N$ with $x=5\%$ and GaN layers is shown in Fig. 2(b), with the interface indicated by arrows. As seen, at 5% Sc composition, there is no strong difference seen in the image between the GaN and $Sc_{0.05}Ga_{0.95}N$ layers, showing that the 5% layer has fairly high crystalline quality with Sc substituting for Ga. However, a slight increase in the contrast variations within the $Sc_{0.05}Ga_{0.95}N$ layer suggests not only the presence of the alloy but also the possibility of a slightly nonuniform distribution of Sc.

As seen in Fig. 2(c), the interface between the 17% Sc-containing layer and the GaN layer is much more obvious. This is due to (1) increased contrast variations within the $Sc_{0.17}Ga_{0.83}N$ layer; and (2) apparent random variations in the stacking sequence of the *c* planes. The contrast variations are interpreted as fluctuations in the Sc alloy concentration, whereas the apparent variations in the stacking sequence are attributed to the incorporation of a number of stacking faults. Since the stacking sequence of hcp GaN and fcc ScN are ABABAB… and ABCABC…; if a layer like C is added to the hcp sequence, a fcc structure is obtained. Therefore, near the transitional regime between the wurtzite GaN and rocksalt ScN—more precisely at Sc concentration 17%—the appearance of stacking faults is natural since the crystal starts to develop toward the more stable rocksalt ScN structure. Nonetheless, the continuation of the *c* planes along the *c* direction clearly remains as the layer grows, which implies that Sc is incorporated into the Ga sublattice even during 3D growth. The Sc does not seem to incorporate into interstitial sites since this would likely lead to greater degradation of the crystal structure or even to an amorphous film.

In Fig. 3 are shown expanded views of the X-TEM images of $Sc_xGa_{1-x}N$ for $x=5\%$ and 17% together with their

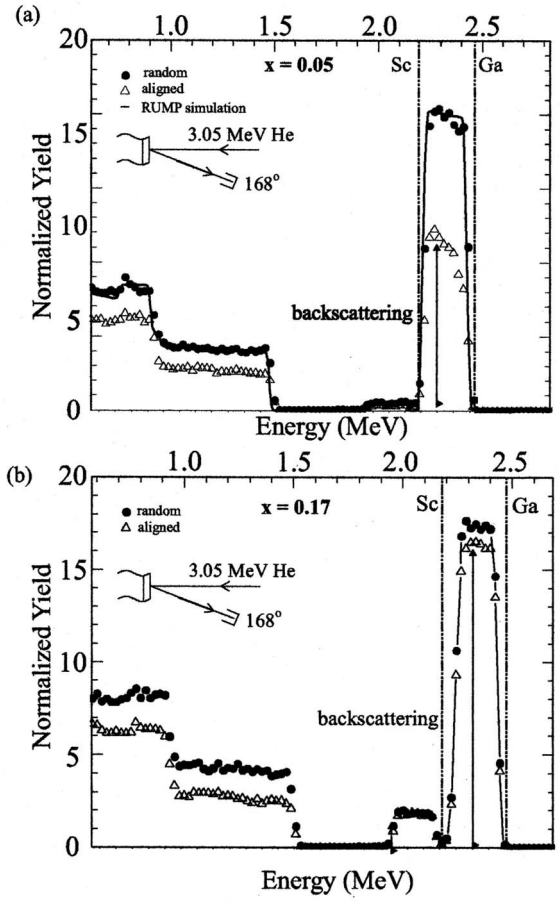


FIG. 4. RBS spectra of $Sc_xGa_{1-x}N$/sapphire(0001) with $x=5\%$ (a), and $x=17\%$ (b).

corresponding fast Fourier transforms (FFT's). The FFT image of $Sc_xGa_{1-x}N$ with $x=5\%$ [Fig. 3(b)] shows a sharp spot pattern, consistent with the real-space image showing a highly crystalline layer. The *out-of-plane* (*y* direction) spacing of the spots is the reciprocal of the *c*-lattice constant, while the *in-plane* (*x* direction) spacing of the spots is the reciprocal of the *a*-lattice constant. Therefore, for the ideal wurtzite structure, the $x:y$ spot spacing ratio should equal $c/a \sim 5.19:3.20=1.62$, and the experimental data are in good agreement with this value.

The FFT image of $Sc_xGa_{1-x}N$ with $x=17\%$ [Fig. 3(d)] shows that the diffraction spots are elongated into horizontal diffraction streaks. This spot elongation indicates only one-dimensional periodicity which is along the *c* direction; the long-range periodicity in the in-plane direction is lost although the short-range periodicity within a single in-plane layer is still seen [Fig. 3(c)]. This loss of long-range in-plane periodicity is consistent with the loss of stacking order seen in the X-TEM image [Fig. 3(c)] which is attributed to the existence of stacking faults.

Shown in Fig. 4 are Rutherford backscattering (RBS) measurements for the $Sc_xGa_{1-x}N$ films with x=5% [Fig. 4(a)] and $x=17\%$ [Fig. 4(b)]. The Sc and Ga signals are each clearly seen in the RBS spectra beginning at the onset energies of 2.2 and 2.45 MeV, respectively. The measured random spectra (black circles) are compared with Rutherford Universal Manipulation Program (RUMP) simulations (black

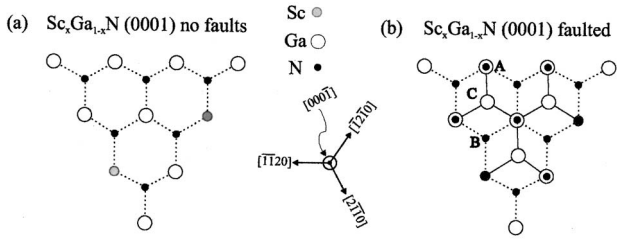


FIG. 5. Schematic models of $Sc_xGa_{1-x}N$ crystal without stacking faults (a), and with stacking faults (b).

lines) for both $Sc_xGa_{1-x}N$/sapphire(0001) films where Sc compositions of $x=5\%$ and 17% were used in the simulations. As can be seen from the RBS spectra of Fig. 4(a), the RUMP fit is quite good, confirming the composition values indicated.

Aligned spectra (open triangles), in which the incident alpha particle beam is aligned with the crystalline *c* axis, indicate the degree of ion crystal channeling; the more elastic backscattering present in the aligned spectrum, the less channeling there is, indicating more backscattering centers in the film. In the case of $Sc_xGa_{1-x}N$ with $x=5\%$ [Fig. 4(a)], the amount of backscattering from Ga and Sc is 54% and 71%, respectively. This significant amount of backscattering in comparison with a pure GaN film (only few % backscattering at most) suggests a large number of scattering centers within the crystalline channels. In the case of $Sc_xGa_{1-x}N$ with $x=17\%$ [Fig. 4(b)], the backscattering from Ga and Sc sites is increased to 94% and 100%, respectively. This indicates an even greater concentration of backscattering centers in the film. In a previous paper,[11] it was supposed that the backscattering of the aligned spectra was attributed to the lattice distortions arising from the incorporation of Sc onto Ga lattice sites. As shown below in our recent theoretical calculations, the lattice distortions are positively found to occur as expected. However, the amount of lattice distortion for $x\sim 6\%$ in ScGaN is found to be only a few degrees at most around any given Sc substitutional site. While the lattice distortions could affect the channeling, it is uncertain whether the cumulative effect of such small distortions would be sufficient to cause the observed backscattering. In the case of the ScGaN film with $x=17\%$, the X-TEM image clearly suggests the presence of stacking faults in the film; stacking faults would increase the number of backscattering sites as a random variation in stacking sequence results in cations blocking otherwise-open channels. This can be understood clearly from Fig. 5(b) where cations incorporating at the faulted sites block the otherwise-open channels.

In the case of $x=5\%$, the X-TEM image did not indicate the presence of many stacking faults; it therefore suggests that either (a) local lattice distortions due to Sc incorporation are surprisingly sufficient to cause significant backscattering; or (b) stacking faults, despite not being observed for 5% Sc concentration in X-TEM, are in fact present in significant quantities in the 5% film. A possible origin of increasing stacking faults with increasing Sc concentration is a reduction in surface diffusion which kinetically limits site sampling during growth, leading to growth of faulted domains. The reduced surface diffusion can be related to the bonding of Sc atoms in comparison with Ga atoms. If one considers that in the ground state, Sc forms 6 bonds with N (rocksalt structure) whereas in the ground state, Ga forms only 4 bonds with N (wurtzite structure), then on a surface, it could be that Sc atoms have more bonds to share with N compared with Ga atoms. Then the N atom will be more likely to bond to the Sc atom site compared to the Ga atom site. This effectively increases the sticking coefficient but decreases the overall surface diffusion and makes it more likely for N atoms to bond at faulted sites. Therefore, as Sc concentration on the surface increases, the probability of forming stacking faults also increases.

To summarize these experimental findings, we observe that ScGaN with small Sc composition in the range 0%–17% can be grown using MBE under N-rich conditions with Sc atoms substituting for Ga atoms. We find that the alloy remains crystalline even at 17% Sc concentration; however, stacking disorder is observed in X-TEM images and confirmed in FFT images. And the backscattering seen in RBS also confirms defects, which are assumed to therefore be stacking faults. Despite these defects, the effect of Sc incorporation on the lattice is to locally distort the lattice, and this effect is not altered despite the presence of the evident stacking faults. In fact, we find that the lattice constants measured are evidently not affected by the stacking faults due to their agreement with the theoretical calculations, as shall be shown below in the theory section. Even though the experimental sample appears to be faulted, the Sc-substitution-induced lattice distortions still occur, as they would even if there were no faults.

## III. THEORY

### A. Theoretical method

To gain a better understanding of the nature of the deformations introduced by Sc atoms in a GaN matrix, we performed first-principles Density Functional Theory calculations using the SIESTA[12] method. These calculations allow us to obtain quantitative information on structural parameters such as lattice constants, bond lengths, and angle values around atomic sites as functions of Sc concentration. Our calculations are done within the local density approximation, using the exchange-correlation potential of Ceperley-Adler[13] as parameterized by Perdew and Zunger.[14] Norm-conserving pseudopotentials of the Troullier-Martins-type,[15] in the Kleinman-Bylander form,[16] are used to remove the core electrons from the calculations. Nonlinear core corrections[17] and relativistic effects were included in the pseudopotential generation. The 3*d* shell in Ga was included in the core. The valence wave functions were expanded on a double-$\zeta$ polarized (DZP) basis set of localized numerical atomic orbitals[18] for all the atoms.

In order to model the structure of the alloys, we performed calculations of wurtzite GaN in supercells containing 32 atoms, in which some of the Ga atoms were substitutionally replaced by Sc. We studied configurations with 0–5 substitutions of Ga by Sc, corresponding to five different concentrations of Sc in the $Sc_xGa_{1-x}N$ alloy ($x=0\%$, 6.25%, 12.50%, 18.70%, and 25%). For each concentration, we con-

sidered a large number of different arrangements of Sc in the lattice. In order to increase the sampling of configurations considered, we did calculations in two different 32-atom supercells: one with rectangular lattice vectors, and another one with hexagonal lattice vectors, producing configurations with different arrangements (periodicity) of the Sc impurities.

A uniform grid with an equivalent plane-wave cutoff of 300 Ry was used to perform the numerical integrations in real space. Integrations over the first BZ were replaced by discrete sums with a *k*-grid cutoff of 12 Å.[19] The systems were relaxed using conjugate gradients until the maximum force on each atom was under 0.04 eV/Å. The supercell vectors were also allowed to relax in order to obtain the equilibrium lattice constants for each of the configurations considered.

### B. Theoretical results

When comparing different configurations for a given Sc concentration, the results are found to be sensitive to the detailed arrangement of the Sc atoms, with differences in energies of the order of 10 meV/atom. Due to the finite size of the supercell used, the sampling of the configurations we have explored does not allow us to extract definitive conclusions about the expected structure of the alloy in thermal equilibrium (degree of order, tendency to segregation, etc.), and it is also clear that growth kinetics may play an important role in the distribution of Sc in the sample. However, the data obtained in our calculations tend to suggest that there is preference for those configurations in which the Sc atoms are distributed uniformly among the different layers along the *c* axis of the crystal. These are the configurations which, for all concentrations, provide the minimum total energies. These are also the configurations which provide the best agreement (concerning the structural parameters, which will be discussed below) with the experimental data. The Sc atoms in different layers tend to be located along close positions in the *a*-*b* plane, in configurations like those shown in Fig. 6 for the hexagonal supercell. We will refer to these configurations as "ordered," in contrast with other, more "random" ones. Our results tend to indicate that these configurations are the most likely to occur during the MBE growth process.

Figure 7 shows the evolution of the calculated lattice parameters *a* and *c* as a function of Sc content. The data represented correspond to the averages of the results obtained for the ordered configurations in the two supercells (hexagonal and rectangular). Both lattice parameters *a* and *c* increase as the Sc concentration is increased. The data show larger changes for the lattice parameter *a* than for *c*, an indication of the existence of anisotropic distortions in the lattice [Note the factor of 4 difference in the *y* scales in Figs. 7(a) and 7(b)]. This result is in good agreement with the experimental observations (data from Ref. 11 also shown in Fig. 7 for comparison). Linear fits of the data yield slopes with a reasonably good agreement between theory and experiment. In the theoretical data, the deviation of the data from the linear fit for the lattice parameter *c* is larger in relative terms, because of the choice of particular configurations with minimum energy, which produces a noise comparable to the variation of the intrinsic change of *c*. However, we clearly see that the theoretical results are able to reproduce qualitatively the different expansion coefficients in the *a* and *c* axes observed in the experiment.

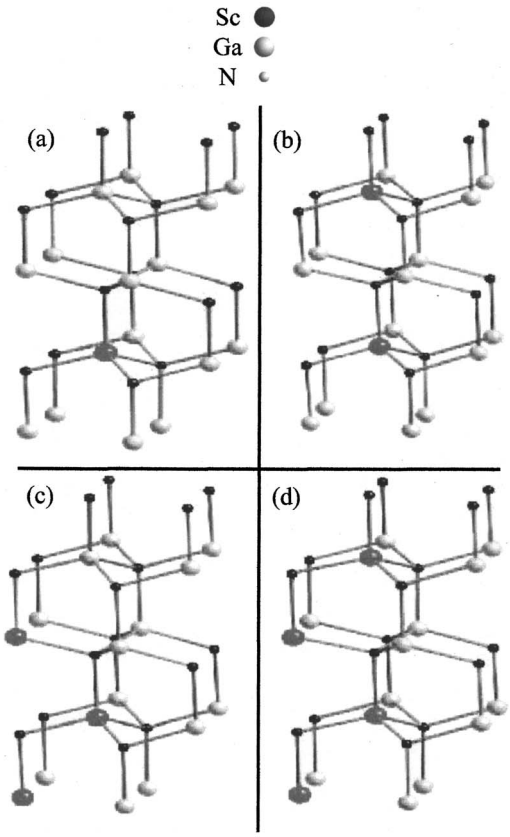


FIG. 6. Examples of ordered configurations for the hexagonal supercell, showing the Sc atoms distributed among different layers along the *c* axis and at nearby positions in the *a*-*b* plane. Each panel shows a different Sc concentration *x*: (a) $x=6.25\%$; (b) $x=12.5\%$; (c) $x=18.7\%$; and (d) $x=25\%$.

Our data also indicate that, for Sc concentrations around 1/4, a qualitative change starts to occur. The *c* lattice parameter starts to *decrease*, in contrast to the increase which occurs for smaller concentrations. This is shown in the last point in Fig. 7(b), and is an indication that, when the alloy incorporates a sufficiently large number of Sc atoms, the structure should evolve towards a layered hexagonal structure, the precursor of a metastable ScN phase predicted by Farrer and Bellaiche.[9] For this phase, $c/a$ is 1.207, much smaller than in the wurtzite phase (1.631), and therefore *c* should decrease with respect to that of wurtzite. The work by Constantin *et al.*[11] provided the first experimental evidence in support of the existence of such phase in this material, showing that, for concentrations larger than 30% this phase is no longer stable and a transition towards the rocksalt structure starts to develop.

To further compare our results with the previous predictions of Farrer and Bellaiche,[9] we performed a calculation with $x=100\%$, by replacing all Ga atoms by Sc atoms in the ideal wurtzite structure. In equilibrium (after relaxation) we obtained the predicted hexagonal layered structure and repro-

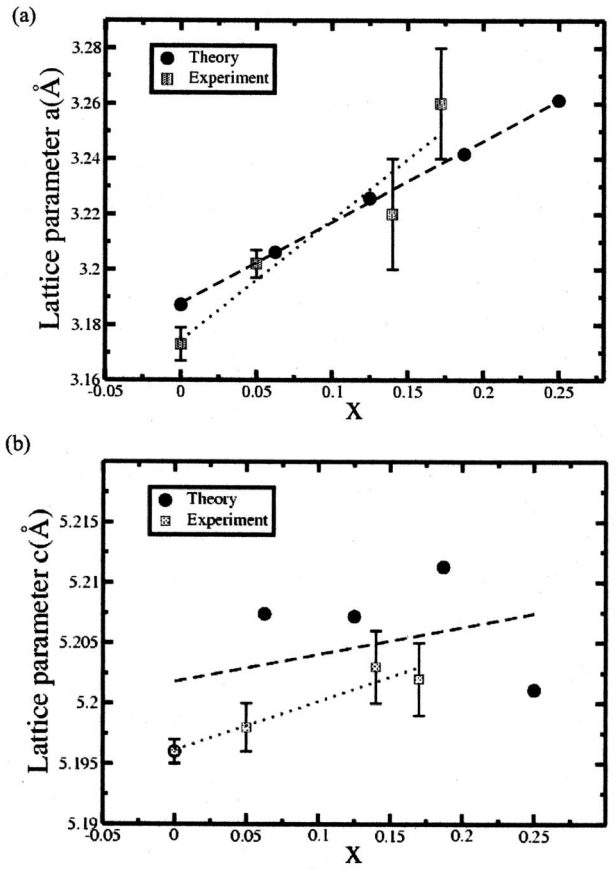


FIG. 7. Lattice parameters $a$ and $c$ as function of Sc concentration $x$. Experimental data are plotted for comparison. For the lattice parameter $c$ the experimental data has been shifted to agree with the known value for GaN. Theory data correspond to the values obtained from ordered configurations. Linear fits are drawn to guide the eye.

duced the decrease in the axial ratio $c/a$ from 1.63 (corresponding to an ideal wurtzite structure) to 1.21 as also obtained by Farrer and Bellaiche.

With the purpose of identifying the mechanisms causing the observed lattice distortions, we studied in detail the changes in bond length and bond angle values for all concentrations and configurations calculated. For ordered configurations values were obtained by averaging over bond lengths and bond angles at different atomic sites for each concentration. For random configurations, the procedure was repeated for all configurations calculated and final values were obtained by further averaging over configurations. In both cases, fluctuations were estimated by standard deviations of the averaged values.

The analysis of bond-length values shows that both Ga-N and Sc-N bond lengths increase with Sc concentration. Analysis of our results, shown in Fig. 8, indicates that, while in ordered configurations the increase is more pronounced for Sc-N bonds than for Ga-N bonds, the opposite occurs for random configurations. As can be seen in Fig. 8, despite some exceptions, there is a tendency to have larger fluctuations in bond length values as Sc concentration increases. These larger fluctuations are also consistent with previous results obtained in GaAsN alloys[20] that show a broadening in the bond-length distribution as N is incorporated into the

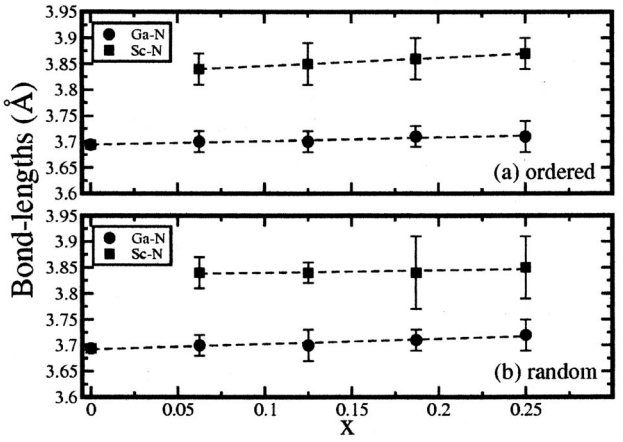


FIG. 8. Bond lengths as function of Sc concentration $x$. (a) Ga-N and Sc-N bond lengths for ordered configurations. (b) Ga-N and Sc-N bond lengths for random configurations. Error bars represent the standard deviation of the average values over the configuration considered.

GaAs matrix. The analysis of angle distortions gives further insight into the formation of an hexagonal layered phase. In-plane and out-of-plane angles (as defined in Fig. 9) show clear deviations from the value of an ideal wurtzite structure $\theta=109.47°$ as the Sc content increases. Our results indicate that in-plane angles deviate towards larger values than the ideal wurtzite value. The relative variations $\Delta\theta/\theta$ between $x=0$ and $x=0.25$ are 0.35%, 1.9%, and 1.1% corresponding to angles around Ga atoms (N-Ga-N), Sc atoms (N-Sc-N) and N atoms (which include Ga-N-Ga, Ga-N-Sc, and Sc-N-Sc angles), respectively. Our results are summarized in Fig. 10. The trend for changes in out-of-plane angles as Sc concentration increases, as appears in Fig. 11, shows a decrease in value as compared with the ideal wurtzite value. The relative variations in this case are −1.22%, −2.0% and −1.8% for N-Ga-N, N-Sc-N, and Ga/Sc–N–Ga/Sc angles, respectively. In both in-plane and out-of-plane cases, distortions around Sc atoms are more pronounced, whereas we obtain larger fluctuations for the values of angles around the N sites. The overall results obtained for variations in in-plane and out-of-plane angles with increased Sc content, indicate a flattening of wurtzite bilayer towards an hexagonal layered structure, in agreement with previous measurements[11] and theoretical predictions.[9]

The conclusion that we draw from the theoretical calculations is that, for the range of Sc concentrations considered, the incorporation of Sc to the lattice produces local distor-

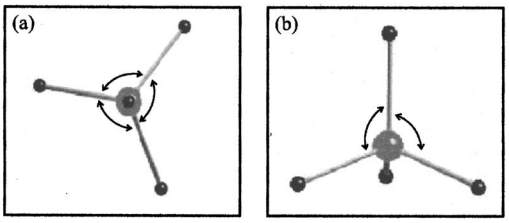


FIG. 9. Angles around atomic sites. (a) In-plane and (b) out-of plane. The notation N-Ga(Sc)-N refers to the angle with vertices at the atomic position of the Ga(Sc) atom. Angles around N-atom sites (Ga/Sc-N-Ga/Sc) were calculated with Ga, Sc or both type of atoms at end positions.

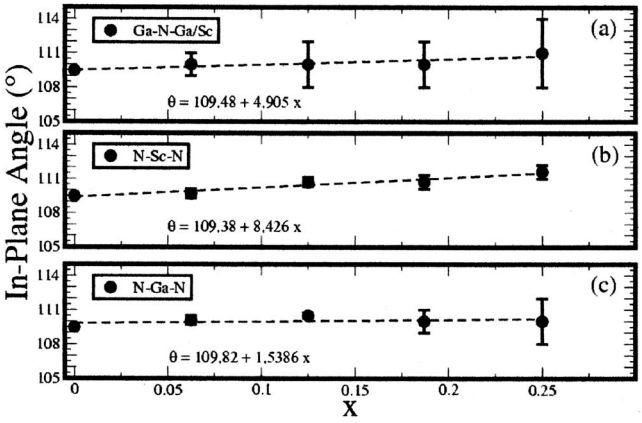


FIG. 10. In-plane angle distortions as a function of Sc concentration $x$ for angles centered at Ga, Sc, and N atomic positions. Linear fits are drawn to guide the eye. Error bars represent the standard deviation of the average values over the configuration considered.

tions that: (i) drive an anisotropic expansion of the lattice vectors, with a larger variation of the in-plane axis, whereas the $c$ axis length increases much less (and eventually decreases for larger Sc concentrations), and (ii) the environment of the Sc atoms tends towards a flattening within the $a$-$b$ plane. Both observations lead to the picture that the wurtzite structure evolves towards the metastable hexagonal ScN phase as more Sc is incorporated into the lattice. Particularly at low Sc concentrations, the deviations of bond lengths and bond angles is relatively small, and therefore the dominant wurtzite structure is preserved at the concentrations considered. This is in agreement with the experimental observations, and in particular with the HRTEM images, which show a small difference in the crystallinity of ScGaN and GaN layers. At larger Sc concentrations, the variations in bond lengths and angles is larger, but our calculations do not allow for the formation of defects (stacking faults) which are clearly observed in the experimental HRTEM images. However, for these concentrations, our calculations have found some configurations in which Sc shows a certain tendency to nucleate in nearby sites, like that shown in Fig. 12. Their energies are only slightly higher than those of the ordered

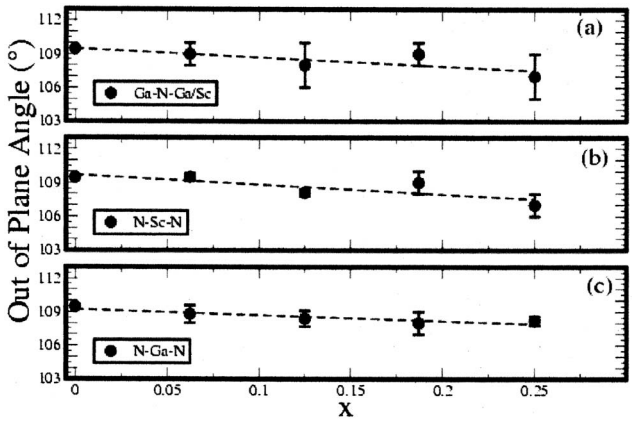


FIG. 11. Out-of-plane angle distortions as a function of Sc concentration $x$ for angles centered at Ga, Sc, and N atomic positions. Linear fits are drawn to guide the eye. Error bars represent the standard deviation of the average values over the configuration considered.

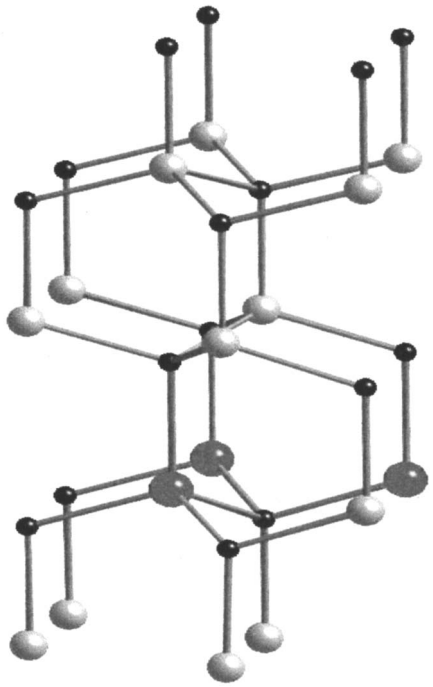

FIG. 12. Configuration for Sc concentration $x$=0.187 with Sc atoms nucleated in plane.

structures, and therefore could play a role. In particular, they could serve as nucleation centers for stacking faults, due to the stress that the segregation of Sc atoms induces in the surrounding GaN lattice. We believe that the presence of nucleation centers for dislocations are an important ingredient for the appearance of stacking faults, since a calculation of the stacking faults energies does not show any significant dependence on the presence of Sc. Their appearance for high Sc content may, therefore, be due to kinetic processes during the growth, or to a mechanism to compensate local stress induced by the nucleation of Sc-rich regions.

## IV. SUMMARY

In summary, we have reported a combined experimental and theoretical study of ScGaN with Sc concentration up to about 17% (experiment) and 25% (theory). The calculations are in overall good agreement with the experiment, and a good match is found between the variation of lattice constants with Sc fraction from experiment vs that from theory. Furthermore, the variation of bond lengths and in-plane and out-of-plane angles as functions of Sc fraction has been studied, and the results agree with a picture in which the addition of Sc to the GaN lattice induces local lattice distortions which tend toward a flattening of the wurtzite bilayer. The experimental evidence shown here also suggests the presence of stacking disorder for the higher Sc fraction (17%). It is likely that kinetic limitations during growth or mechanisms of stress release in Sc-rich regions may be the cause of the stacking disorder. Despite this disorder, the lattice constants of the 17% sample appear to be entirely determined by the local lattice distortions (and not by the stacking defects), as also predicted by the theory.

[1]P. Dismukes, W. M. Yim, and V. S. Ban, J. Cryst. Growth **13/14**, 365 (1972).
[2]J. P. Dismukes and T. D. Moustakas, Proc.-Electrochem. Soc. **96–11**, 110 (1996).
[3]D. Gall, I. Petrov, L. D. Madsen, J.-E. Sundgren, and J. E. Geene, J. Vac. Sci. Technol. A **16**, 2411 (1998).
[4]D. Gall, I. Petrov, N. Hellgren, L. Hulman, J.-E. Sundgren, and J. E. Geene, J. Appl. Phys. **84**, 6034 (1998).
[5]T. D. Moustakas, R. J. Molna, and J. P. Dismukes, Proc.-Electrochem. Soc. **96–11**, 197 (1996).
[6]A. R. Smith, H. A. H. Al-Brithen, D. C. Ingram, and D. Gall, J. Appl. Phys. **90**, 1809 (2001).
[7]H. A. AL-Brithen, A. R. Smith, and D. Gall, Phys. Rev. B **70**, 045303 (2004).
[8]M. G. Moreno-Armenta, L. Mancera, and N. Takeuchi, Phys. Status Solidi B **238**, 127 (2003).
[9]N. Farrer and L. Bellaiche, Phys. Rev. B **66**, 201203(R) (2002).
[10]M. E. Little and M. E. Kordesch, Appl. Phys. Lett. **78**, 2891 (2001).
[11]C. Constantin, H. Al-Brithen, M. B. Haider, D. Ingram, and A. R. Smith, Phys. Rev. B **70**, 193309 (2004).
[12]J. Soler, E. Artacho, J. Gale, A. García, J. Junquera, P. Ordejón, and D. Sánchez-Portal, J. Phys.: Condens. Matter **14**, 2745 (2002).
[13]D. M. Ceperley and B. J. Adler, Phys. Rev. Lett. **45**, 566 (1980).
[14]S. Perdew and A. Zunger, Phys. Rev. B **32**, 5048 (1981).
[15]N. Troullier and J. L. Martins, Phys. Rev. B **43**, 1993 (1991).
[16]L. Kleiman and D. M. Bylander, Phys. Rev. Lett. **48**, 1425 (1982).
[17]S. G. Louie, S. Froyen, and M. L. Cohen, Phys. Rev. B **26**, 1738 (1982).
[18]E. Artacho, D. Sánchez-Portal, P. Ordejón, A. García, and J. M. Soler, Phys. Status Solidi B **215**, 809 (1999).
[19]J. Moreno and J. Soler, Phys. Rev. B **45**, 13891 (1992).
[20]G. Ciatto, F. d'Acapito, S. Sanna, V. Fiorentini, A. Polimeni, M. Capizzi, S. Mobilio, and F. Boscherini, Phys. Rev. B **71**, 115210 (2005).